Bilayer infiltration system combines benefits from both coarse and fine sands promoting nutrient accumulation in sediments and increasing removal rates

N. Perujo,[a,b,c*] A.M. Romaní,[c] and X. Sanchez-Vila[a,b]

[a] Department of Civil and Environmental Engineering, Universitat Politècnica de Catalunya (UPC), Jordi Girona 1-3, 08034 Barcelona, Spain

[b] Hydrogeology Group (UPC−CSIC), Barcelona, Spain

[c] GRECO - Institute of Aquatic Ecology, Universitat de Girona, 17003 Girona, Spain

*Corresponding author: nuria.perujo@upc.edu

TOC graphic

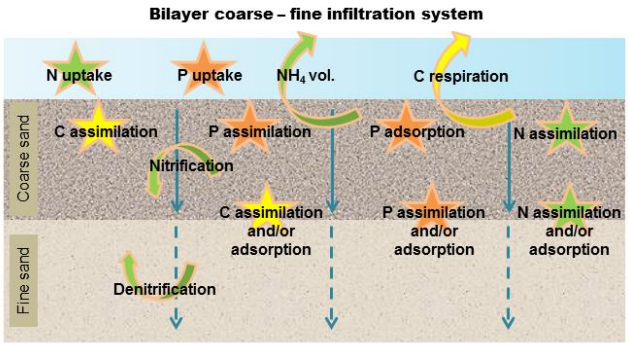

Abstract

Infiltration systems are treatment technologies based on water percolation through porous media where biogeochemical processes take place. Grain size distribution (GSD) acts as a driver of these processes and their rates, as well as it influences nutrient accumulation in sediments. Coarse sands inhibit anaerobic reactions such as denitrification and could constrain nutrient accumulation in sediments due to smaller specific surface area. On the other hand, fine sands provide higher nutrient accumulation but need a larger

area available to treat the same volume of water; furthermore they are more susceptible to bio-clogging. Combining both sand sizes in a bilayer system would allow infiltrating greater volume of water and the occurrence of aerobic/anaerobic processes. We studied the performance of a bilayer coarse-fine system compared to a monolayer fine one –by triplicate- in an outdoor infiltration experiment to close the C-N-P cycles simultaneously in terms of mass balances. Our results confirm that the bilayer coarse-fine GSD promotes nutrient removal by physical adsorption and biological assimilation in sediments, and further it enhances biogeochemical process rates (two-fold higher than the monolayer system). In overall, the bilayer coarse-fine system allows treating larger volume of water per surface unit achieving similar removal efficiencies as the fine system.

1. Introduction

High nutrient loads into freshwater ecosystems lead worldwide to eutrophication, associated harmful algal blooms, and "dead zones" due to hypoxia (1). In urban areas, the input of nutrients from wastewater treatment plants (WWTP) into freshwaters can contribute to eutrophication processes especially in areas characterized by flow intermittency (2). However, biogeochemical dynamics are affected by numerous factors which hinder the understanding of physical, chemical and biological dynamics related to the potential nutrient removal of water bodies (3). The implementation of infiltration systems in WWTPs before pouring water into streams is considered as a way to decrease nutrient load inputs to rivers, thus diminishing river eutrophication especially during low flow periods (4). Infiltration systems are water treatment technologies that rely on fluid percolation through a porous medium where a combination of biological, chemical, and physical processes help improving the quality of the influent water during the infiltration path (5).

The grain size distribution (GSD) of the porous medium is an important characteristic for infiltration systems (6-8). GSD, mostly linked to the pore size distribution and connectivity, modulates the distribution and transport of terminal electron acceptors, nutrients and organic matter in depth (7-8), and acts as a driver of the biogeochemical processes and their rates (9). Also, substrate grain size influences wastewater compounds' adsorption (10). On one hand, coarse, well-sorted sediments imply large permeability values that result in high dissolved oxygen (DO) concentrations in depth, promoting aerobic processes such as nitrification, but inhibiting anaerobic reactions which are of great importance for the complete total dissolved nitrogen (TDN) removal (11). Furthermore, coarse sediments enhance high loads

of nutrients and organic matter which are associated with high biogeochemical rates but with low advection times (12). However, coarse sediments could constrain compounds' adsorption due to smaller specific surface area (13). On the other hand, in fine sediments, the low DO supply through infiltration drives anoxic conditions, where bacteria catalyze full denitrification (14). It is also known that fine sand has larger specific surface area and high adsorbing capacity (15-16) but lower permeability which can constrain wastewater treatment (17) since the risk of substrate clogging may increase (13). Considering all this, it is difficult to assess which substrate size is better to use since both grain sizes display benefits and drawbacks. Accordingly, Perujo et al. (12) carried out an experiment with the aim of deepening in the relationship between physicochemical and biological parameters in different GSDs and results suggested that a bilayer coarse-fine system may integrate the positive aspects of coarse sands and those of fine sands. Kauppinen et al. (18) studied the performance of multi-layered sand filters but focusing mainly on pathogens removal and using combinations of 0-8 mm sand, 0-2 mm biotite and 2-4 mm which showed no different performance between them in terms of nutrients removal. Latrach et al. (19) used a multi-soil-layering system which consisted of a matrix of permeable material (mainly gravel) with soil mixture "boxes" composed of coarse and fine sand, silt and clay, resulting in a high permeable system used to treat raw wastewater, but without carrying out a comparison on amongst system designed with different grain size distributions.

The study of biogeochemical processes in sand filters is relatively complex and several processes are involved in the transformation and removal of carbon, nitrogen and phosphorous compounds (20). We are not aware of any work aimed at studying the relevance of a bilayer coarse-fine grain size distribution compared to a monolayer fine sand system to close the C-N-P cycles simultaneously, thus quantifying all the biogeochemical pathways of C, N and P occurring both in the interstitial water and in the sediment surfaces. The main objective of this research is to compare the performance of a bilayer coarse-fine sand system with that of a monolayer fine sand–in triplicate- in an outdoor infiltration experiment and specifically, to study (i) the distribution of biogeochemical processes in the depth profile, (ii) the importance of nutrient accumulation in sediments in regards to adsorption and assimilation processes; and (iii) the link of biogeochemical process rates to removal efficiencies at each system, in order to decipher whether the bilayer system optimizes the performance of infiltration systems. To achieve these objectives, we move away from qualitative process' description, and rely on quantification based on measurements (sampling of interstitial water and sediment and analysis of chemical species in depth from in-situ

replicated tanks during 104 days) and validated by means of mass balance evaluations in depth as well as the study of C:N:P molar ratios in sediments to further understand nutrient accumulation processes in sediments.

2. Material and methods

2.1 Experimental setup

An outdoor infiltration experiment was performed with secondary treated municipal wastewater. Physicochemical parameters of the infiltrated water and nutrient loadings are described in Table S1. Two flow-through sand tank systems (three replicates per system) were created using different GSDs: (1) a bilayer Coarse-Fine (CF) system, consisting of a 20 cm layer of coarse sand (0.9 – 1.2 mm) placed on top of a 20 cm layer of fine sand (0.075 – 0.250 mm); and (2) a monolayer Fine (F) system, with 40 cm of fine sand (0.075 – 0.250 mm) (Fig. S1). Sands were bought from a company dealing (and selling) aggregates (Adicat Tribar, S.L.). They consisted of siliceous sand, rounded shape, free from clays and organic matter and with low metal contents (Al_2O_3 < 0.5 % of the sand dry weight, Fe_2O < 0.04 %, CaO < 0.05 %, and K_2O < 0.5 %). Both systems consisted of tanks of 0.21 m^3 capacity and 0.46 m^2 of infiltration surface area; in the upper part of each one, a valve was used to ensure a constant water level creating a constant surface water layer and a continuous infiltration in each system. At the bottom of each tank a gravel layer was placed to facilitate drainage of water towards the outlet to resemble vertical infiltration conditions. There was no water recirculation in the experiment. Three water ports were installed in the wall of the tanks; at depths 4, 18 and 38 cm. The experiment was performed during 104 days from April to July 2016. Outdoor temperature was 21.6 ºC on average (21) and 234 mm of accumulated rainfall (22) during the time the experiment ran. Sunlight conditions were allowed only in the surface of the tanks, to mimic real infiltration basins. Since the accumulated rainfall only represented 0.12 % and 0.26 % of the daily infiltrated water in our systems (CF and F, respectively) we consider that the effect of rainfall was negligible. Hydraulic parameters of each system as well as organic and nutrient loadings are detailed in Table S1.

Water and sediments (note that we use the term “sediment” to refer to the porous media (sand) which is being colonized by biofilm) were sampled weekly at the start and biweekly at the end of the experiment, for a total of 9 sampling campaigns. Samples were collected at about the same time (11 – 12 am), and with consistent weather conditions (sunny, with no registered precipitations two days previous to

sampling) to minimize variability due to environmental factors. Water samples were collected from the inlet water, the surface pond, and the three water ports installed at each tank. Dissolved nutrient and organic carbon concentrations were analyzed for all samples.

Sediment sampling was performed using a sediment core sampler (Eijkelkamp 04.23.SA) to a depth of 40 cm and each core was subdivided in three specific depth layers (0-4 cm as "surface sediment", 18-22 cm as "20 cm depth sediment" and 36-40 cm as "40 cm depth sediment"). Each sample was homogenized, and then subsamples of 1 cm^3 of sediment were collected using an uncapped syringe, and kept frozen (-20 ºC) until analysis to determine nutrient and carbon content within the sediments. After taking each sediment core, one methacrylate empty column was placed at the same place to avoid the collapse of the surrounding sediment in the tanks, in an attempt to minimize the disruption of the flow field.

2.2 Water analysis

Samples for dissolved nutrients and dissolved organic carbon (DOC) were filtered in pre-combusted (4h, 450 ºC) filters (GF/F, 0.7 µm, Whatmann). After filtering, dissolved nutrients were analyzed in fresh, while DOC samples were acidified and kept at 4 ºC until analysis. DOC concentrations were determined using a total organic carbon analyzer (TOC-V_{CSH} Shimadzu). For inorganic nutrient determination, samples were filtered again (Nylon filters, 0.2 µm, Whatmann) and analyzed as follows: NO_x - as the sum of NO_2^- and NO_3^- - by ionic chromatography (761 Compact IC 1.1 Metröhm), and NH_4 by the spectrophotometric sodium salicylate protocol (23). Total dissolved nitrogen (TDN) and total dissolved phosphorous (TDP) samples were digested before analysis. The digestion protocol (adapted from Koroleff (24)) consisted in an oxidation where the reagent prepared in NaOH solution (0.375 M) containing $K_2S_2O_8$ (0.18 M) and H_3BO_3 (0.48 M) was added (2 ml) to filtered samples (20 ml) in tightly capped Pyrex glass tubes. Tubes were closed, shaken and autoclaved (90 min, 115 ºC). Absorbance was measured at 275 and 220 nm for TDN determination. TDP determination followed the protocol from Murphy and Riley (25). Dissolved organic nitrogen (DON) was calculated as the difference between TDN and inorganic nitrogen ($DON = TDN - (NH_4 + NO_x)$).

2.3 Sediment analysis

For carbon and nitrogen determination in sediments, distilled Milli-Q water (1.5 ml) was added to each sediment sample, then sonicated for 1 minute and shook. Aliquots of the extract (100 µl) were pipetted into pre-weight tin cups and placed in the oven at 60 ºC until drying. The remaining extract was kept at 4

ºC. Pipetting was repeated five times to obtain a final dry weight of ca. 1 - 3 mg. Tin cups were weighted and sediment carbon and nitrogen content were analyzed in a CN-analyzer (Carlo Erba).

The protocol used for P determination in sediments is adapted from Aspila et al. (26). The samples were dried at 50 ºC, crushed and accurately weighted. Samples for total phosphorous (P_{tot}) determination were transferred into porcelain crucibles, ignited in a muffle furnace (550 ºC for 1h, following Andersen (27)), and then let to cool for one hour. Samples for total phosphorous and inorganic phosphorous (P_{inorg}) determinations were transferred to 100 ml Erlenmeyer flasks with HCl acid (1.0 M, 25 ml). Mixtures were boiled for 15 minutes on a hot plate, filtered (Whatmann, 2.5 µm) to separate the liquid phase from the sediment, and ten-fold diluted with Milli-Q water. P_{tot} and P_{inorg} were determined by the Molybdate-blue method (25). P_{org} was determined by colorimetry, as the difference between P_{tot} and P_{inorg}. The ratio between P_{inorg} /P_{org} was calculated as an indicator of the proportion of inorganic phosphorous accumulated in sediments versus the organic phosphorous in sediments, where values >1 indicate dominance of inorganic P and values < 1 indicate dominance organic P. Sediment molar C:N:P ratios were also calculated.

2.4 Removal rates, removal efficiencies and mass balances

2.4.1 Removal rates

Biogeochemical transformation rates were calculated for different chemical species both in water and sediment. Data were transformed to homogeneous units to allow the comparison between the rates measured in water and in sediment. Total water nutrient loads were calculated at each sampling depth (surface water layer, 4 cm, 18 cm and 38 cm) for all the duration of the experiment, and balances between each two consecutive sampling points were calculated. The results were divided by the total duration of the experiment (104 days) and by the spatial volume of each layer. Data from the sediments were calculated separately for each depth (surface, 20 cm, and 40 cm), multiplied by the conversion factor (1.45 g DW-Dry Weight- per cm^3) and divided by 104 days. All values are reported in $\mu g \cdot cm^{-3} \cdot day^{-1}$. Negative rates indicate a removal process.

2.4.2 Removal efficiencies

Removal efficiencies were calculated from the nutrient loads following equation 1. Two calculations were performed: 1) from the inlet to the outlet, and 2) from the surface of the sediment to the outlet, this one to

exclude processes occurring in the layer of surface water and to focus on the processes occurring in the sediment.

$$\text{Removal efficiency (\%)} = 100 \cdot (\text{inlet-outlet})/\text{inlet}, \quad (1)$$

where, inlet – outlet are the nutrient loads (expressed in $mg \cdot day^{-1}$).

2.4.3 Mass balances

Mass balances were calculated from the removal rates and results are reported for different depth infiltration layers (see Figure S1): top layer (includes water mass balance from surface water to 4 cm depth and the C-N-P contents measured in the surface sediment); mid layer (includes water mass balance from 4 cm to 18 cm depth and the sediment C-N-P contents measured at 20 cm depth); and finally, the bottom layer (includes water mass balance from 18 to 38 cm depth and the sediment C-N-P contents measured at 40 cm depth). As the potential processes occurring in the layer of surface water include complex biological (photosynthesis, planktonic uptake of nutrients, organic matter transformation) and chemical (photochemical) reactions that were not monitored, mass balances from inlet water to surface water were not assessed.

2.4.3.1 Carbon mass balances

It is assumed that the main DOC removal pathways are depth dependent. In the upper infiltration layer, the main C transformation pathways are C respiration (C_{resp}) and C accumulation in sediments (C_{sed}), and the mass balance can be expressed as:

$$C_{DOC\ inlet} - C_{sed} - C_{resp} = C_{DOC\ outlet} \quad (2)$$

In depth, for the mid and bottom layers, transformation pathways are related to C used in denitrification (C_{denitr}), aside from respiration and accumulation in sediments (28). Nonetheless, as the two terms C_{resp} and C_{denitr} were not directly measured in the deeper layers, they were considered as a single term, denoted as $C_{resp/denitr}$, so that the mass balance equation can be written as:

$$C_{DOC\ inlet} - C_{sed} - C_{resp/denitr} = C_{DOC\ outlet} \quad (3)$$

2.4.3.2 Nitrogen mass balances

It is assumed that the main nitrogen transformation pathways are depth dependent: (i) TDN removal pathways in the top infiltration layer are driven by NH_4 volatilization (29) and N accumulation in sediments; (ii) in depth TDN removal pathways consist of denitrification to N gas (30) and N

accumulation in sediments (31). Furthermore, (iii) DON can be mineralized to NH_4 (32); (iv) in depth NO_x can be transformed to DON (33). Also, (v) under oxic conditions NH_4 is nitrified to NO_x (32); (vi) in depth NO_x can be denitrified to N_2 (14) or reduced to NH_4 (34).

According to these assumptions, N mass balances are described. TDN mass balances are given by equation 4 for the top infiltration layer and 5 for the mid and bottom ones. The main N removal paths are NH_4 volatilization (denoted in the equations as $TDN_{NH4\ volat}$), N being accumulated in sediments ($TDN_{N\ sed}$), and NO_x denitrification ($TDN_{NOx\ denitr}$).

$$TDN_{inlet} - TDN_{NH4\ volat} - TDN_{N\ sed} = TDN_{outlet} \quad (4)$$

$$TDN_{inlet} - TDN_{N\ sed} - TDN_{NOx\ denitrification} = TDN_{outlet} \quad (5)$$

Ammonium mass balances are given by equation 6 for the top layer and 7 for the mid and bottom ones. Positive contributions on NH_4 mass balances are the DON being mineralized to NH_4 (denoted by $NH_{4\ DON\ mineral}$), and the NO_x being reduced to NH_4 ($NH_{4\ NOx\ reduction}$). Negative contributions on ammonium mass balance are the NH_4 that is being transformed to DON ($NH_{4\ DON\ prod}$), the one that left the system via volatilization ($NH_{4\ volat}$), the one being nitrified to NO_x ($NH_{4\ nitrif}$), and that accumulated in the sediment ($NH_{4\ N\ sed}$).

$$NH_{4\ inlet} + NH_{4\ DON\ mineral} - NH_{4\ volat} - NH_{4\ nitrif} - NH_{4\ N\ sed} = NH_{4\ outlet} \quad (6)$$

$$NH_{4\ inlet} + NH_{4\ NOx\ reduction} - NH_{4\ DON\ prod} - NH_{4\ N\ sed} = NH_{4\ outlet} \quad (7)$$

In parallel, NO_x mass balances are given by equation 8 for the top infiltration layer (where there is a net production) and equation 9 for the mid and bottom ones (with a net reduction). Positive contribution on NO_x mass balances include NH_4 being nitrified to NO_x ($NO_{x\ prod}$). The negative terms in the mass balance equations include the NO_x leaving the system via denitrification ($NO_{x\ denitr}$), that transformed to NH_4 via reduction ($NO_{x\ reduction}$ -in the text called DNRA-), and the NO_x being transformed to DON ($NO_{x\ DON\ prod}$).

$$NO_{x\ inlet} + NO_{x\ prod} = NO_{x\ outlet} \quad (8)$$

$$NO_{x\ inlet} - NO_{x\ denitr} - NO_{x\ reduction} - NO_{x\ DON\ prod} = NO_{x\ outlet} \quad (9)$$

2.4.3.3 Phosphorous mass balances

For the phosphorus mass balances, the assumption is that the TDP removal pathways at any depth are driven by phosphorous content in sediments, $TDP_{P\ sed}$ (6). Thus, the TDP mass balance equation is written as follows:

$$TDP_{inlet} - TDP_{P\,sed} = TDP_{outlet} \quad (10)$$

Where $TDP_{P\,sediment}$ can be also expressed as the sum of phosphorous adsorption in sediments, $TDP_{P\,inorg}$ and phosphorous assimilation, $TDP_{P\,org}$, resulting in the following mass balance equation:

$$TDP_{inlet} - TDP_{P\,inorg} - TDP_{P\,org} = TDP_{outlet} \quad (11)$$

2.5 Data Analysis

Dissolved nutrient concentrations and DO were analyzed by repeated measures ANOVA (factors: depth and system, $p < 0.05$). Data for each system were further analyzed separately through Tukey post-hoc analysis to detect significant different groups in depth. The parameters measured in sediments (C, N and P) were analyzed by covariance ANCOVA (factors: depth and system, $p < 0.05$) and further analyzed using the Bonferroni post-hoc test to detect significant different groups in depth and significant differences between systems at each depth. P_{inorg}/P_{org} ratios were also analyzed (ANOVA, factor: depth and system, $p < 0.05$) and the Tukey post-hoc analysis was then applied to all systems separately (factor: depth). Removal rates and removal efficiencies were subject to an ANOVA analysis to detect differences between systems at a given depth and for the overall systems (factor: system, $p < 0.05$). All statistical analyses have been performed using R software (R version 3.1.1, Stats Package).

3. Results

3.1 Distribution of chemical species in depth

Concentrations of dissolved chemical species measured at each depth are shown in Figures S2 - S5. Both systems showed an increase in DOC, DON and DO concentrations in the surface water layer compared to those in the inlet water. In the surface water layer, there was also a slight decrease in the concentrations of NH_4, NO_x and TDP for the F system. These slight changes from the inlet water to the surface water layer (although not being statistically significant) resulted in higher NO_x and TDP concentrations in the surface water in the CF system; and higher DO concentration in the F one. A decrease in DOC and DON concentrations was observed in the top sediment layer (surface to 5 cm depth). TDN concentrations gradually decreased in depth, but higher values were measured in CF at 20 cm, as compared to those in F. NH_4 and NO_x concentration profiles in depth were similar in both systems; NH_4 concentration decreased at 5 cm depth but then increased. Oppositely, NO_x concentration increased at 5 cm depth but then decreased. The F system displayed higher NH_4 and lower NO_x concentrations at 20 cm depth, as

compared to CF. Both systems displayed a similar pattern for the TDP concentration profile, with a decrease from the surface to 5 cm depth and then stabilization. Higher TDP concentrations were reported in the CF system in the surface and at 20 and 40 cm depth than in the F system. DO concentrations decreased with depth, with lowest values found in the F system at 20 and 40 cm depth.

C, N and P concentrations in sediments (Figure 1) were higher in the surface than in the deep layers. The CF system showed higher inorganic P concentration in the surface sediment than F, while for total phosphorous no significant differences between systems were detected. At depths 20 and 40 cm, C, N, inorganic P and total P concentrations in sediments were significantly higher in the CF system than in F. The ratio P_{inorg}/P_{org} (Table S2) decreased significantly in depth indicating higher accumulation of organic P than inorganic P in deeper sediments in both systems. In the surface, the CF system showed significantly higher P_{inorg}/P_{org} ratio than the F one. Sediment molar ratios are described as follows, in the top layer both systems showed similar C:N ratio (≈ 7.8 -7.6), $N:P_{org}$ ratio (≈ 14.7 – 17.7), and $C:P_{org}$ ratio (≈ 115 – 146). In the mid layer, C:N ratio increased slightly in both systems (≈ 8.3 – 9), and $N:P_{org}$ ratio decreased (≈ 4.2 – 3.1) as well as $C:P_{org}$ ratio (≈ 35.8 – 22.7). Molar ratios in the bottom layer are similar than in the mid layer, C:N ratio (≈ 10.2 – 9.0), $N:P_{org}$ ratio (≈ 2.7 – 4.3) and $C:P_{org}$ ratio (≈ 23.8 – 32.5 in CF and F, respectively).

3.2 Carbon, nitrogen and phosphorus mass balances

3.2.1 Carbon mass balances

Carbon mass balances per unit volume of sediment at each sediment layer are described in Figure 2. Removal rates decreased in depth in both systems. In the top layer, DOC removal and C respiration rates were largest in CF while C accumulation rates in sediments were similar between GSDs. This resulted in C accumulation in sediments accounting for 25.1 % and 50.3 % of the DOC removal in CF and F, respectively. Thus, respiration resulted in the main C removal path in the CF system (74.9 %), while in the F one an equal contribution of C accumulation and C respiration to the global DOC balance was found (50.3 % and 49.7 %, respectively). In the middle infiltration layer, both systems were estimated to receive unaccounted C inputs as DOC balances were positive; for this reason, we could not estimate the relative contribution of each carbon removal pathway in that layer, however greatest C accumulation rate in sediments was found in CF. In the bottom layer (20 to 40 cm depth), greatest C accumulation rate was found in CF but similar C respiration rates were described in both systems. In this layer, C_{sed} accounted

for 19.1 % and 17.3 %, while $C_{resp/denitr}$ accounted for 80.9 % and 82.7 % of the total DOC removed in the CF and F systems, respectively.

3.2.2 Nitrogen mass balances

Nitrogen mass balances per unit volume of sediment are described in Figure 3. In general, process rates decreased in depth in both systems. In the top infiltration layer, ammonium volatilization was estimated as the main TDN removal path (92.4 % in CF and 90.7 % in F) while N accumulation in the surface sediments accounted for 7.6 % (CF) and 9.3 % (F) of the TDN removal. Notice that only small amounts of N were unaccounted for (3.0 and 0.7 $\mu g\ N \cdot cm^{-3} \cdot day^{-1}$ for CF and F, respectively). In the mid and bottom layers, denitrification was estimated to be the main TDN removal pathway in both systems (90 – 95 %) while N accumulation in sediments accounted for only 2 – 10 %. Other N transformation pathways were estimated in the infiltration systems: DON mineralization to NH_4, and NH_4 nitrification to NO_x in the top infiltration layer; DNRA and NO_x transformation to DON in the middle one, and DNRA in the bottom one.

The contributions of these processes in the general balance of intermediate species of N (NH_4 and NO_x) vary between GSDs. Thus, in CF we find that with regard to NH_4 transformation in the upper layer, dominates nitrification (65%). Regarding NO_x transformation in this system, in the middle layer dominates the transformation to DON (43%) and denitrification (55%) and in the lower layer dominates DNRA (72%). However, in the F system, in the top layer dominates both nitrification and ammonium volatilization (≈ 50% each), in the middle layer dominates DNRA (43%) and denitrification (60%), and in the bottom layer dominates denitrification (80 %). Mass balance closure discrepancies in the mid and bottom layers were very low (0.17 - 0.25 and 0.41 – 0.44 $\mu g\ N \cdot cm^{-3} \cdot day^{-1}$ for CF and F, respectively).

3.2.3 Phosphorous mass balances

Mass balances of the P species per unit volume of sediment are described in Figure 4. We assumed that all TDP removed was accumulated in the sediment through adsorption or assimilation. However, in some of the mass balance evaluations, TDP removal was lower than P accumulated in sediments, potentially indicating an unaccounted P input. From Total P accumulated in sediments, proportions between organic and inorganic P were calculated; in surface sediments, results suggested similar accumulation of inorganic P (49 %) and organic P (51 %) in CF, while accumulation of organic P (60 %) contributed more than inorganic P (40 %) in F. At 40 cm depth, organic P accumulation accounted for higher proportion (56 – 63 %) compared to inorganic P (37 – 44 %) in both systems. Higher TDP and P accumulation rates

were measured in the top infiltration layer. Comparing systems, TDP removal rate was higher in CF in top and bottom layers and P accumulation rate was higher in the CF system in the mid infiltration layer.

3.3 Removal efficiencies

We report in Table 1 the removal efficiencies of each infiltration system. Considering only the layers that constitute the sediments, both systems showed similar DOC (7 - 11 %), TDN (18 – 23 %) and TDP (14 – 16 %) removal efficiencies, but higher TDP and TDN removal rates were reported in CF as compared to F. Including the processes in the full system (three sediment layers plus the surface water layer), the F system resulted in higher TDP removal efficiency (23 %), compared to the CF (12 %).

4. Discussion

Our data support that biogeochemical processes of C-N-P species are depth and GSD dependent, both in qualitative (most relevant processes) and in quantitative terms. As expected, highest rates occurred in the top layer which might be controlled by high nutrient, and DO and electron acceptors availability as well as higher biomass developed in surface sediments compared to deeper ones (35). Regarding our results, nutrient accumulation in the top layer sediments played a key role on nutrient removal efficiencies, especially for DOC and TDP removals (representing up to 50% of their respective removal, while N accumulation in sediment represents 10% of its removal). This removal is suggested to be mainly due to biological processes (assimilation) since the C:N:P elemental molar ratios (calculated from total C and N and organic P in sediments) are close to the known Redfield ratio described for autotrophic biomass (106:16:1, Redfield (36)). Interestingly, even though we expected higher nutrient accumulation rates in the fine sediment due to higher surface area available in fine compared to coarse sediments (37), both systems showed similar rates. Furthermore, in the case of P, where we distinguished the inorganic to the organic fraction, inorganic P showed greater accumulation in the bilayer coarse-fine system. This contradiction could be due to the fact that difference in sediment texture has mostly been associated with the presence of silts and clays (< 2 μm) (38) and in our study the presence of silts and clays was excluded. Furthermore, higher inorganic P accumulation measured in the bilayer system could be related to higher TDP concentrations in the surface water layer (39) which could enhance physical adsorption of inorganic P. It is also worth noting that we are not comparing coarse and fine sands, but GSDs where the bilayer coarse-fine system does not act like coarse homogeneous sediment since physical characteristics such as K and flow velocity are lower than a coarse sediment (12) and therefore both GSDs the bilayer coarse-

339 fine and the monolayer fine systems promote the removal of nutrients through the accumulation of these
340 nutrients in the sediments via adsorption and assimilation.

341 Other significant biogeochemical processes occurring in the top layer of infiltration systems are mostly
342 related to nitrogen (ammonium volatilization and the coupled processes of nitrification and DON
343 mineralization) but also include carbon respiration. As expected, C respiration, nitrification and DON
344 mineralization rates were approximately double in the bilayer system compared to the monolayer system
345 which would indicate that those rates could be proportional to input loads. Greater attention should be
346 focused on ammonium volatilization as it is the main TDN removal pathway in the aerobic top layer of
347 infiltration systems and it seems to be independent of input loads. Ammonium volatilization is a
348 physicochemical process driven by temperatures higher than 20 ºC and pH ranging 6.6-8.0 (40) for this
349 reason showed similar rates in both systems.

350 In depth, accumulation of nutrients in sediments was less relevant as a removal path to that observed for
351 the top layer. The slight increase in C:N sediment molar ratios as well as the decrease in $C:P_{org}$ and $N:P_{org}$
352 ratios compared to the top sediment layer could be linked to the fact that the dominant living biomass in
353 depth is microbial biomass which showed a different elemental molar ratio than autotrophic biomass.
354 Cleveland and Liptzin (41) stated C:N:P = 60:7:1 as the elemental molar ratio for microbial biomass.
355 According to this, sediment molar ratios at 20 and 40 cm depth following the elemental molar ratio
356 described for microbial biomass could be indicative of nutrient assimilation as a main pathway of nutrient
357 accumulation in sediments in depth, but also they could be linked to physical adsorption of microbial
358 biomass that is being transported from upper to lower sediment layers. Specifically, higher accumulation
359 rates in the interface of the bilayer system could be linked to physical entrapment of microbial biomass
360 when reaching the transition from the coarse to the fine sediment layers, as well as retention of carbon,
361 nitrogen and phosphorous species which are then potential to be biologically assimilated or physically
362 adsorbed. At the same time, the imbalance of the molar ratios to a greater accumulation of organic P (low
363 $C:P_{org}$ and $N:P_{org}$ ratios) suggests the deposition of dead organic matter and the accumulation and
364 adsorption of P in lower layers where the mineralization processes of this organic matter could possibly
365 be limited by reduced microbial activity and lower DO. We further contend that unaccounted C inputs
366 reported in the experiment at intermediate depths were probably due to the generation of microbial
367 soluble products (42), or to desorption of organic carbon retained in top sediments (43). Similarly,
368 unaccounted P inputs in mass balances at intermediate depths could be related to the release of

phosphates previously assimilated in upper layers by bacteria and algae following their death and subsequent degradation (44).

In depth, TDN concentration is the only parameter decreasing in the mid and bottom layers mainly due to anaerobic processes such as denitrification that could take place even in DO concentrations of around 4 mg $O_2 \cdot L^{-1}$ (45). Larger loading inputs could explain the larger denitrification rates reported in the bilayer system which resulted in higher TDN removal rates especially in the mid layer as compared to the monolayer fine one. However, sediment GSD in depth modulated N transformation pathways. Specifically, the larger C accumulation in the interface between the coarse and fine layer in CF could favor the conversion of NO_x to DON, most relevant in organic horizons (33). NO_x transformation to DON has been mainly attributed to abiotic processes (46) and specific DON reactions remain unknown. Interestingly, at 40 cm depth, DNRA dominated over denitrification in the CF system, while the opposite happened in the F system. Higher hydraulic conductivity in the former system could have favored interstitial DO transport in depth (11), driving the high DO concentration measured at 20 and 40 cm depth, and being the reason for DNRA being the dominant pathway in depth compared to denitrification (under oxic conditions the denitrification/DNRA ratio is low, Roberts et al. (47)). In this study, different contributions of N transformation pathways between the bilayer and the monolayer systems did not affect the overall TDN removal efficiencies, possibly due to the fact that main differences were achieved in the mid and bottom layers where N concentrations and transformation rates were far smaller than in the top ones.

To complete the picture, some comments can be made regarding biogeochemical processes occurring in the surface water layer. Although the observed changes were small, these may have implications in the global nutrient balance in infiltration systems. The most significant changes were the increase in DOC and DON concentrations, related to the potential release of soluble microbial products and algal exudates (48-49), and combined with NH_4, NO_x and TDP concentrations decrease, these associated with possible nutrient uptake by planktonic microorganisms and algae (50-51). Photosynthetic activity in the surface water layer might be responsible for DO concentration increase (52) which, in turn, favours nitrification in the top sediment layer due to high DO concentration in infiltrated water (nitrification has high DO requirements: 4.57 g of O_2 per gram of NH_4, Tchobanoglous (53)).

Biogeochemical processes occurring in the surface water layer seem to be directly related to the hydraulic retention time (HRT). This should be interpreted carefully since, as large HRT could favor TDN and TDP removal efficiencies in monolayer fine systems, it could also decrease DOC removal efficiency.

Biogeochemical rates - influenced by GSDs - have implications on removal efficiencies in infiltration systems. Main processes related to DOC, TDN and TDP removals are located in the top sediment layer and include C respiration and assimilation, NH_4 volatilitzation, as well as P assimilation and adsorption. On one hand, the bilayer coarse-fine system allows to infiltrate greater volume of water, and so greater input nutrient loads, than the monolayer fine system. This results in greater rates of biogeochemical processes that are dependent on input loads such as C respiration in the bilayer system. Furthermore, in the bilayer coarse-fine system the convergence of characteristics such as grain size distribution and advection times allows to achieve higher TDN and TDP removal rates in the bilayer, as well as similar or even higher (if comparing values in the interface) nutrient accumulation rates in sediments through physical adsorption and biological assimilation, compared to the monolayer system. Overall, the bilayer coarse-fine system allows to treat a larger volume of water per surface unit achieving similar removal efficiences as the monolayer fine one.

ACKNOWLEDGEMENTS

We acknowledge support from TRARGISA – Depuradora de Girona, especially to Cristina and Lluís. Also we acknowledge Betty for her support in the lab. This work was supported by the Spanish Ministry of Economy and Competitiveness (GL2014-58760-C3-2-R and project ACWAPUR - PCIN-2015–239), the ERA-NET Cofund Waterworks 2014, the Department of Universitats, Recerca i Societat de la Informació de la Generalitat de Catalunya, and the European Social Fund.

Supporting Information. Scheme of the two systems used in the experiment; physicochemical parameters measured at the inlet water hydraulic parameters and input loads of each infiltration sand system used; boxplots of dissolved species measured at different depths at each system (DOC, TDN, NO_x, NH_4, DON, TDP and DO) and ratios between inorganic and organic P measured in the sediment.

References

1. Diaz, R. J.; Rosenberg, R. Spreading dead zones and consequences for marine

ecosystems. *Science* **2008**, 321 (5891), 926-929; DOI 10.1126/science.1156401.

2. Martí, E.; Riera, J. L.; Sabater, F. Effects of wastewater treatment plants on stream nutrient dynamics under water scarcity conditions. In *Water scarcity in the mediterranean*; Sabater, S., Barceló, D., Eds.; Springer: Berlin, Heidelberg 2009; pp173-195.
3. Pai, H.; Villamizar, S. R.; Harmon, T. C. Synoptic Sampling to Determine Distributed Groundwater-Surface Water Nitrate Loading and Removal Potential Along a Lowland River. *Water Resources Research* **2017**, 53 (11), 9479-9495; DOI 10.1002/2017WR020677.
4. Fox, P. *Soil Aquifer Treatment for sustainable water reuse;* AWWA Research Foundation and American Water Works Association, Denver, CO, 2001.
5. Dillon, P.; Page, D.; Vanderzalm, J.; Pavelic, P.; Toze, S.; Bekele, E.; Sidhu, J.; Prommer, H.; Higginson, S.; Regel, R.; Rinck-Pfeiffer, S.; Purdie, M.; Pitman, C.; Wintgens, T. A critical evaluation of combined engineered and aquifer treatment systems in water recycling. *Water Sci. Technol.* **2008**, 57, 753–762; DOI 10.2166/wst.2008.168.
6. Brix, H.; Arias, C. A.; del Bubba, M. Media selection for sustainable phosphorus removal in subsurface flow constructed wetlands. *Water Sci. Technol.* **2001**, 44, 47–54.
7. Boulton, A. J.; Findlay, S.; Marmonier, P.; Stanley, E. H.; Valett, H. M. The Functional Significance of the Hyporheic Zone in Streams and Rivers. *Annu. Rev. Ecol. Syst.* **1998**, 29, 59–81.
8. Nogaro, G.; Datry, T.; Mermillod-Blondin, F.; Descloux, S.; Montuelle, B. Influence of streambed sediment clogging on microbial processes in the hyporheic zone. *Freshw. Biol.* **2010**, 55, 1288–1302; DOI 10.1111/j.1365-2427.2009.02352.x.
9. Baker, M. A.; Vervier, P. Hydrological variability, organic matter supply and denitrification in the Garonne River ecosystem. *Freshw. Biol.* **2004**, 49, 181–190; DOI 10.1046/j.1365-2426.2003.01175.x.
10. Ren, Y. X.; Zhang, H.; Wang, C.; Yang, Y. Z.; Qin, Z.; Ma, Y. Effects of the substrate depth on purification performance of a hybrid constructed wetland treating domestic sewage. *J. Environ. Sci. Heath A* **2011**, 46, 777-782.
11. Mueller, M.; Pander, J.; Wild, R.; Lueders, T.; Geist, J. The effects of stream substratum texture on interstitial conditions and bacterial biofilms: Methodological strategies. *Limnologica* **2013**, 43, 106–113; DOI 10.1016/j.limno.2012.08.002.

12. Perujo, N.; Sanchez-Vila, X.; Proia, L.; Romaní, A. M. Interaction between Physical Heterogeneity and Microbial Processes in Subsurface Sediments: A Laboratory-Scale Column Experiment. *Environ. Sci. Technol*. **2017**, 51, 6110–6119; DOI 10.1021/acs.est.6b06506.
13. Wu, H. M.; Zhang, J.; Ngo, H. H.; Guo, W. S.; Hu, Z.; Liang, S.; Fan, J. L.; Liu, H. A review on the sustainability of constructed wetlands for wastewater treatment: design and operation. *Bioresour. Technol*. **2015**, 175, 594-601.
14. Dong, L. F.; Smith, C. J.; Papaspyrou, S.; Stott, A.; Osborn, A. M.; Nedwell, D. B. Changes in Benthic Denitrification, Nitrate Ammonification, and Anammox Process Rates and Nitrate and Nitrite Reductase Gene Abundances along an Estuarine Nutrient Gradient (the Colne Estuary , United Kingdom). *Appl. Environ. Microbiol.* **2009**, 75, 3171–3179; DOI 10.1128/AEM.02511-08.
15. Huang, X.; Liu, C.; Wang, Z.; Gao, C.; Zhu, G.; Liu, L. The Effects of Different Substrates on Ammonium Removal in Constructed Wetlands: A Comparison of Their Physicochemical Characteristics and Ammonium-Oxidizing Prokaryotic Communities. *Clean Soil Air Water* **2013**, 41, 283–290.
16. Meng, J.; Yao, Q.; Yu, Z. Particulate phosphorus speciation and phosphate adsorption characteristics associated with sediment grain size. *Ecol. Eng*. **2014**, 70, 140–145; DOI 10.1016/j.ecoleng.2014.05.007.
17. Zhao, Z.; Chang, J.; Han, W.; Wang, M.; Ma, D.; Du, Y.; Qu, Z.; Chang, S. X.; Ge., Y. Effects of plant diversity and sand particle size on methane emission and nitrogen removal in microcosms of constructed wetlands. *Ecol. Eng*. **2016**, 95, 390-398.
18. Kauppinen, A.; Martikainen, K.; Matikka, V.; Veijalainen, A. M.; Pitkänen, T.; Heinonen-Tanski, H.; Miettinen, I. T. Sand filters for removal of microbes and nutrients from wastewater during a one-year pilot study in a cold temperate climate. J. *Environ. Manage.* **2014**, 133, 206-213.
19. Latrach, L.; Ouazzani, N.; Masunaga, T.; Hejjaj, A.; Bouhoum, K.; Mahi, M.; Mandi, L. Domestic wastewater disinfection by combined treatment using multi-soil-layering system and sand filters (MSL–SF): A laboratory pilot study. *Ecol. Eng*. **2016**, 91, 294-301.
20. Achak, M.; Mandi, L.; Ouazzani, N. Removal of organic pollutants and nutrients from olive mill wastewater by a sand filter. *J. Environ. Manage.* **2009**, 90(8), 2771-2779.

21. AEMET - State Agency of Meteorology. Ministry of the Environment and Rural and Marine Affairs, Spanish Government. (AEMET - Agencia Estatal de meteorología. Ministerio de Medio Ambiente y Medio Rural y Marino, Gobierno de España) Website; http://www.aemet.es/es/serviciosclimaticos/ vigilancia_clima/analisis_estacional (accessed Feb 12, 2017).
22. Meteocat - Meteorological Service of Catalonia. Department of Territory and Sustainability, Government of Catalonia. (Meteocat - Servei meteorològic de Catalunya. Departament de Territori i Sostenibilitat, Generalitat de Catalunya) Website; http://www.meteo.cat/wpweb/serveis/ peticions-de-dades/peticio-dinformes-meteorologics (accessed Feb 12, 2017).
23. Reardon, J.; Foreman, J. A.; Searcy, R. L. New reactants for the colorimetric determination of ammonia. *Clin. Chim. Acta* **1966**, 14, 403–405; DOI 0.1016/0009-8981(66)90120-3.
24. Koroleff, F. Simultaneous oxidation of nitrogen and phosphorus compounds by persulfate. *Methods seawater Anal.* **1983**, 2, 205–206.
25. Murphy, J.; Riley, J. A modified single solution method for the determination of phosphate in natural waters. *Anal. Chim. Acta* **1962**, 27, 31–36.
26. Aspila, K.; Agemian, H.; Chau, A. S. A Semi-automated Method for the Determination of Inorganic , Organic and Total Phosphate in Sediments. *Analyst* **1976**, 101, 187–197.
27. Andersen, J. M. An Ignition Method for Determination of Total Phosphorus in Lake Sediments. *Water Res.* **1976**, 10, 329–331.
28. Abel, C. D. T.; Sharma, S. K.; Mersha, S. A.; Kennedy, M. D. Influence of intermittent infiltration of primary effluent on removal of suspended solids, bulk organic matter, nitrogen and pathogens indicators in a simulated managed aquifer recharge system. *Ecol. Eng.* **2014**, 64, 100–107; DOI 10.1016/j.ecoleng.2013.12.045.
29. Reddy, G. B.; Hunt, P. G.; Phillips, R.; Stone, K.; Grubbs, A. Treatment of swine wastewater in marsh-pond-marsh constructed wetlands. *Water Sci. Technol*. **2001**, 44, 545 – 550.
30. Reddy, K. R.; D'Angelo, E. M. Biogeochemical indicators to evaluate pollutant removal efficiency in constructed wetlands. *Water Sci. Technol*. **1997**, 35, 1–10; DOI 10.1016/S0273-1223(97)00046-2.
31. Bitton, G. Role of microorganisms in biogeochemical cycles. In *Wastewater microbiology*;

514 Bitton, G., Ed.; John Wiley and Sons: New Jersey 1999; pp 75-105.
515 32. Ruane, E. M.; Murphy, P. N. C.; French, P.; Healy, M. G. Comparison of a Stratified and a
516 Single-Layer Laboratory Sand Filter to Treat Dairy Soiled Water from a Farm-Scale Woodchip
517 Filter. *Water. Air. Soil Pollut*. **2014**, 225, 1–10; DOI 10.1007/s11270-014-1915-z.
518 33. Dail, D.B.; Davidson, E. A.; Chorover, J. Rapid abiotic transformation of nitrate in an acid forest
519 soil. *Biogeochemistry* **2001**, 54, 131–146.
520 34. Tiedje, J. M. Ecology of denitrification and dissimilatory nitrate reduction to ammonium. In
521 *Environmental Microbiology of Anaerobes*; Zehnder, A. J. B., Ed.; John Wiley and Sons: New
522 York 1988; pp 179–244.
523 35. Freixa, A.; Rubol, S.; Carles-Brangarí, A.; Fernàndez-Garcia, D.; Butturini, A.; Sanchez-Vila,
524 X.; Romaní, A. M. The effects of sediment depth and oxygen concentration on the use of organic
525 matter: An experimental study using an infiltration sediment tank. *Sci. Tot. Env*. **2016**, 540, 20-
526 31.
527 36. Redfield, A. C. The biological control of chemical factors in the environment. *American scientist*
528 **1958**, 46(3), 230A-221.
529 37. Zhu, H.; Wang, D.; Cheng, P.; Fan, J.; Zhong, B. Effects of sediment physical properties on the
530 phosphorus release in aquatic environment. *Science China Physics, Mechanics & Astronomy*
531 **2015**, 58(2), 1-8.
532 38. Liu, Q.; Liu, S.; Zhao, H.; Deng, L.; Wang, C.; Zhao, Q.; Dong, S. The phosphorus speciations
533 in the sediments up-and down-stream of cascade dams along the middle Lancang River.
534 *Chemosphere* **2015**, 120, 653-659.
535 39. Del Bubba, M.; Arias, C. A.; Brix, H. Phosphorus adsorption maximum of sands for use as
536 media in subsurface flow constructed reed beds as measured by the Langmuir isotherm. *Water*
537 *Res*. **2003**, 37(14), 3390-3400.
538 40. Poach, M.; Hunt, P.; Reddy, G.; Stone, K.; Matheny, T.; Johnson, M. H.; Sadler, E. J. Ammonia
539 Volatilization from Marsh-Pond-Marsh Constructed Wetlands. *J. Environ. Qual*. **2004**, 33, 844–
540 851.
541 41. Cleveland, C.C.; Liptzin, D. C: N: P stoichiometry in soil: is there a "Redfield ratio" for the
542 microbial biomass? *Biogeochemistry* **2007**, *85*(3), 235-252.
543 42. Essandoh, H. M. K.; Tizaoui, C.; Mohamed, M. H. A. Removal of dissolved organic carbon and

nitrogen during simulated soil aquifer treatment. *Water Res*. **2013**, 47, 3559–3572; DOI 10.1016/j.watres.2013.04.013.

43. Quanrud, D. M.; Hafer, J.; Karpiscak, M. M.; Zhang, J.; Lansey, K. E.; Arnold, R. G. Fate of organics during soil-aquifer treatment: sustainability of removals in the field. *Water Res*. **2003**, 37, 3401–3411.
44. Essandoh, H. M. K.; Tizaoui, C.; Mohamed, M. H. A.; Amy, G.; Brdjanovic, D. Soil aquifer treatment of artificial wastewater under saturated conditions. *Water Res*. **2011**, 45, 4211–4226; DOI 10.1016/j.watres.2011.05.017.
45. Gao, H.; Schreiber, F.; Collins, G.; Jensen, M. M.; Kostka, J. E.; Lavik, G.; de Beer, D.; Zhou, H.; Kuypers, M. M. Aerobic denitrification in permeable Wadden Sea sediments. *ISME J*. **2010**, 4, 417–426; DOI 10.1038/ismej.2010.166.
46. Rückauf, U.; Augustin, J.; Russow, R.; Merbach, W. Nitrate removal from drained and reflooded fen soils affected by soil N transformation processes and plant uptake. *Soil Biol. Biochem*. **2004**, 36, 77–90; DOI 10.1016/j.soilbio.2003.08.021.
47. Roberts, K. L.; Kessler, A. J.; Grace, M. R.; Cook, P. L. M. Increased rates of dissimilatory nitrate reduction to ammonium (DNRA) under oxic conditions in a periodically hypoxic estuary. Geochim. *Cosmochim. Acta* **2014**, 133, 313–324; DOI 10.1016/j.gca.2014.02.042.
48. Czerwionka, K. Influence of dissolved organic nitrogen on surface waters. *Oceanologia* **2016**, 58, 39–45; DOI 10.1016/j.oceano.2015.08.002.
49. Sieczko, A.; Maschek, M.; Peduzzi, P. Algal extracellular release in river-floodplain dissolved organic matter: Response of extracellular enzymatic activity during a post-flood period. *Front. Microbiol.* **2015**, 6, 1–15; DOI 10.3389/fmicb.2015.00080.
50. Hein, M.; Pedersen, M. F.; Sand-Jensen, K. Size-dependent nitrogen uptake in micro- and macroalgae. *Mar. Ecol. Prog. Ser*. **1995**, 118, 247–253.
51. Kirchman, D. L. The uptake of inorganic nutrients by heterotrophic bacteria. *Microb. Ecol.* **1994**, 28, 255–271; DOI 10.1007/BF00166816.
52. Drapcho, C. M.; Brune, D. E. The partitioned aquaculture system : impact of design and environmental parameters on algal productivity and photosynthetic oxygen production. *Aquac. Eng.* **2000**, 21, 151–168.
53. Tchobanoglous, G. Fundamentals of biological treatment. In *Wastewater Engineering:*

574 *Treatment and Reuse*; Tchobanoglous, G., Burton, F.L., Stensel, H.D., Eds.; Metcalf & Eddy
575 Inc: New York 2003; pp 611–635.

576

Figures

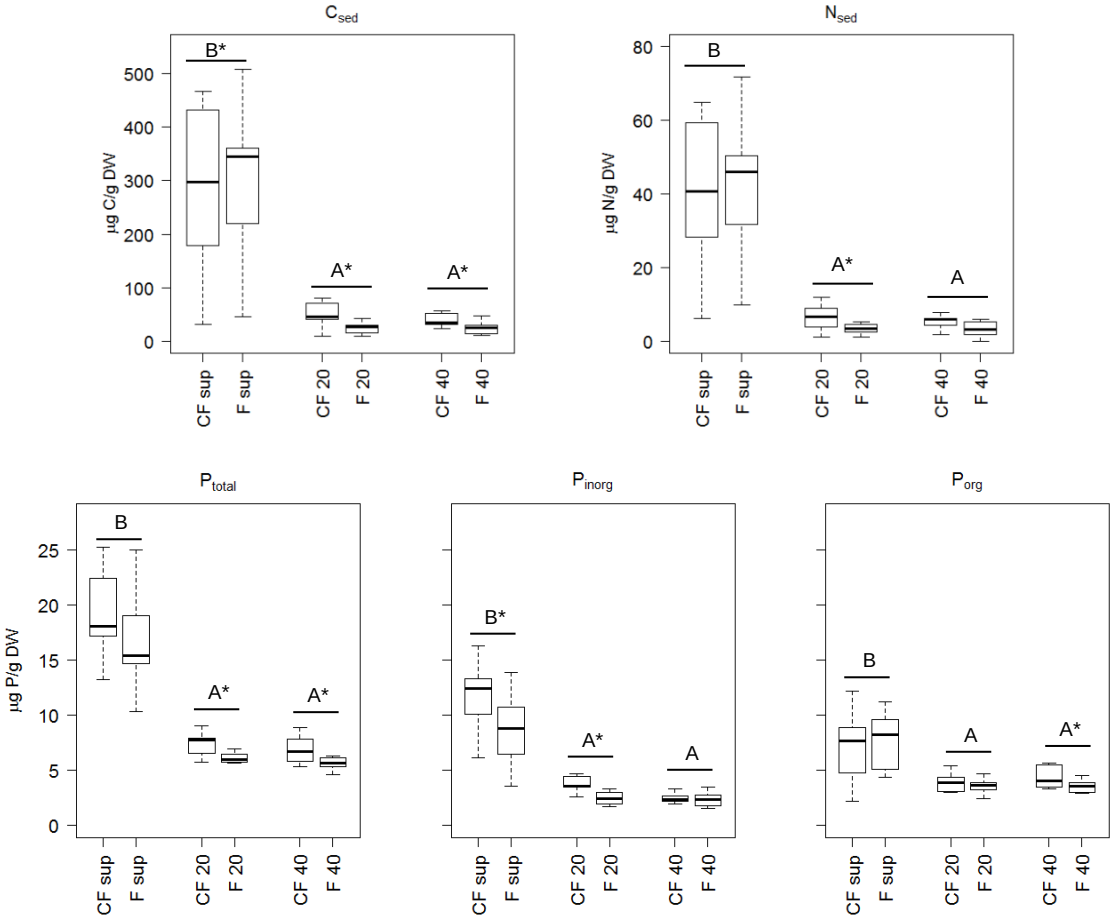

Figure 1 Boxplots for carbon, nitrogen and phosphorous species (total P, inorganic P and organic P) concentrations measured in sediments as a function of depth (sup: superficial, 20: 20 cm depth, 40: 40 cm depth) and GSDs (CF: bilayer coarse-fine system; F: monolayer fine system) and Tukey's post-hoc analysis after ANCOVA analysis for depth ($p < 0.05$). Asterisks determine differences between GSDs at each given depth (ANCOVA, $p < 0.05$).

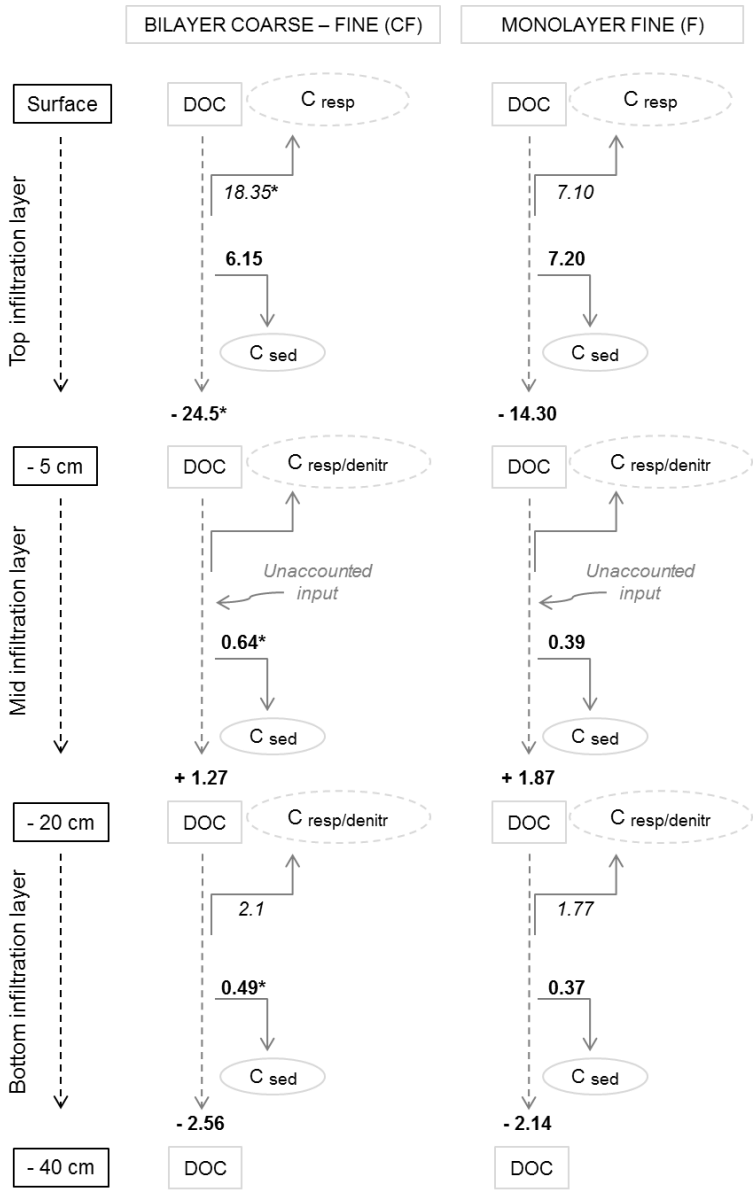

Figure 2 Carbon mass balances for the main C transformation processes and removal paths in the sediment layers. Values in **bold** indicate mass balances calculated from experimental data while values in *italic* are parameters estimated through equations 2 and 3. Asterisk indicates significant difference between systems (ANOVA, factor: system, $p < 0.05$). Dotted oval circles refer to dissolved species that leave the system via gas; solid line oval circles refer to dissolved species that are being accumulated in the sediment. Results are expressed as µg $C \cdot cm^{-3} \cdot day^{-1}$. Negative values indicate dissolved components removal.

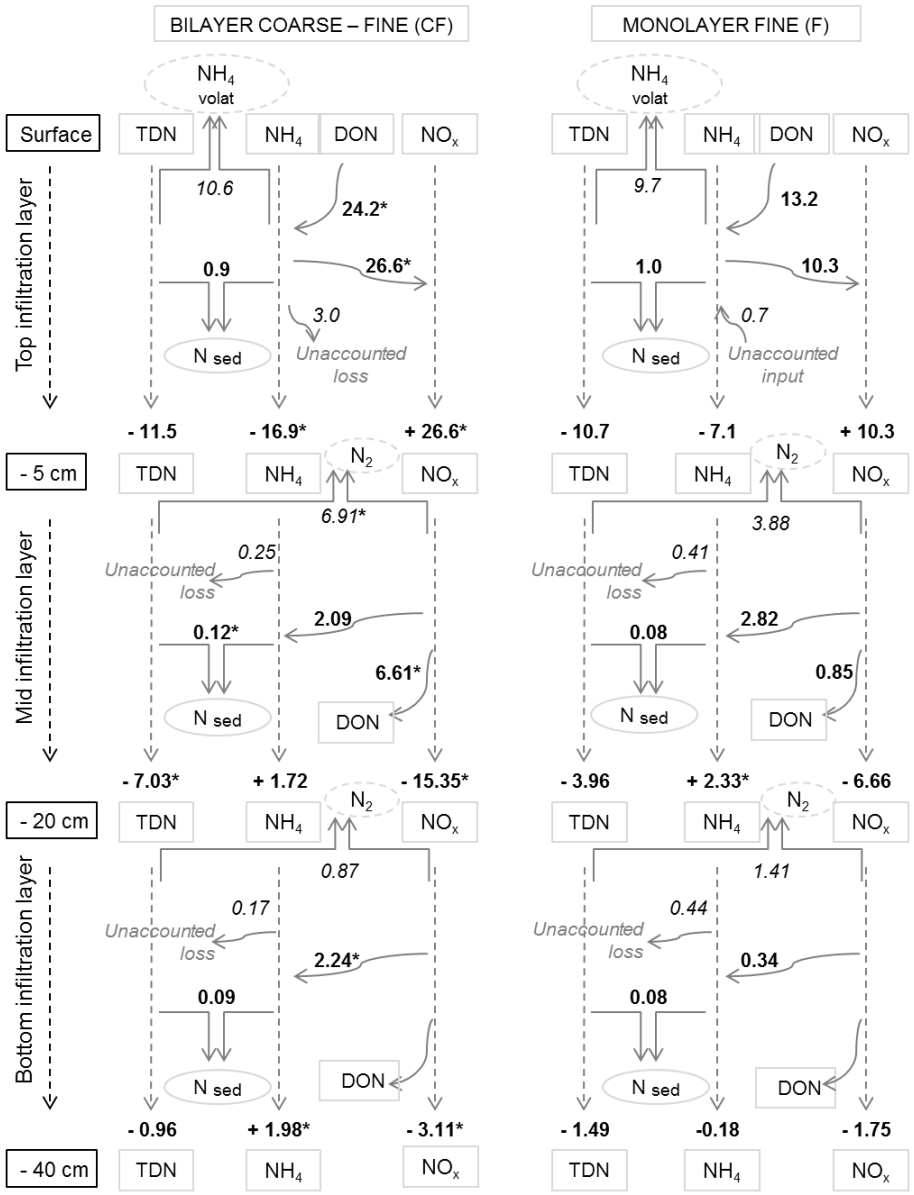

Figure 3 Nitrogen mass balances for the main N transformation processes and removal paths in the sediment layers. Values in **bold** indicate mass balances calculated from experimental data while values in *italic* are parameters estimated through equations 4-9. Asterisk indicates significant difference between systems (ANOVA, factor: system, $p < 0.05$). Dotted oval circles refer to dissolved species that leave the system via gas; solid line oval circles refer to dissolved species that are being accumulated in the sediment. Results are expressed as µg N·cm-3·day-1. Negative values indicate dissolved components removal. DON balances in the bottom layer resulted in low and highly uncertain values, and so, they were excluded from mass balance calculations.

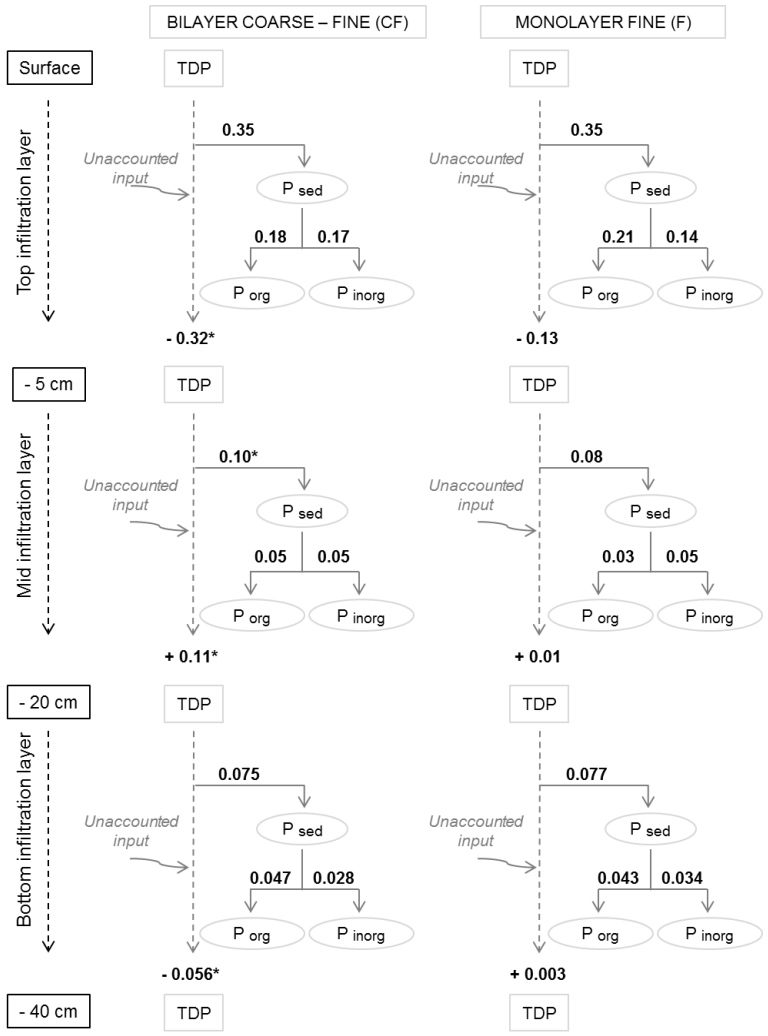

Figure 4 Phosphorous mass balances for the main P transformation processes and removal paths in the sediment layers. Values in **bold** indicate mass balances calculated from experimental data while values in *italic* are parameters estimated through equations 10 and 11. Asterisk indicates significant difference between systems (ANOVA, factor: system, $p < 0.05$).Solid line oval circles refer to dissolved species that are being accumulated in the sediment. Results are expressed as $\mu g\ P \cdot cm^{-3} \cdot day^{-1}$. Negative values indicate dissolved components removal.

Tables

Table 1 Removal efficiencies (%) and overall removal rates measured in the infiltration systems

		Surface – 40 cm depth		Inlet – 40 cm depth	
		CF	F	CF	F
DOC	%	7.44 ± *2.7*	11.31 ± *1.8*	5.50 ± *4.5*	6.53 ± *2.0*
	Removal rate	-3.87 ± *1.1*	-2.15 ± *0.4*		
TDN	%	18.45 ± *3.1*	23.03 ± *2.6*	17.23 ± *2.7*	22.75 ± *4.2*
	Removal rate	**-4.55 ± *0.5***	-3.57 ± *0.2*		
TDP	%	13.91 ± *3.0*	16.46 ± *5.4*	11.87 ± *2.6*	**25.67 ± *4.3***
	Removal rate	**-0.027 ± *0.005***	-0.011 ± *0.002*		

Removal rates are expressed as µg $C \cdot cm^{-3} \cdot day^{-1}$ for DOC, µg $N \cdot cm^{-3} \cdot day^{-1}$ for TDN and µg $P \cdot cm^{-3} \cdot day^{-1}$ for TDP. Considering only the sediment part of the systems (three infiltration layers) correspond to the column "Surface – 40 cm depth", while removal efficiencies for the whole system, including the surface water layer correspond to the column "Inlet – 40 cm depth". Values in bold indicate the system with significant higher value of the specified parameter comparing systems (ANOVA, factor: system, $p < 0.05$).